THE EFFECTS OF RADIATION, DIET, AND MICROGRAVITY ON COLONOCYTE GENE EXPRESSION

An Undergraduate Research Scholars Thesis

by

RYAN JOSEPH BINDEL

Submitted to the Undergraduate Research Scholars program at
Texas A&M University
in partial fulfillment of the requirements for the designation as an

UNDERGRADUATE RESEARCH SCHOLAR

Approved by Research Advisor: Dr. Nancy Turner

May 2017

Major: Biomedical Science

TABLE OF CONTENTS

ABSTRACT

The Effect of Radiation, Diet, and Microgravity on Colonocyte Gene Expression

Ryan J. Bindel
Department of Veterinary and Biomedical Science
Texas A&M University

Research Advisor: Dr. Nancy Turner
Department of Nutrition and Food Science
Texas A&M University

Recent progress has been made in understanding the physiological responses to conditions prevalent in the space flight environment, including radiation source, duration of radiation exposure, weightlessness, and diet. The aim of this project was to use an experimental model simulating the space environment to investigate the immune response with exposure to oxidative stress, weightlessness, and continuous low dose ionizing radiation. Mice were randomly assigned to groups according to a 2 x 2 x 2 factorial design of continuous cobalt (^{60}Co) radiation (C-RAD) or no radiation (SHAM), weight bearing or hind limb unloaded, and a diet with high or normal iron levels. The mice (n=50) were given a 45 or 650 mg iron/kg diet, and maintained in a full body head down tilt for 42 days during the radiation treatment phase. Continuous radiation (C-RAD) mice were exposed to a whole-body dose of ^{60}Co gamma (γ) radiation on a continuous basis (0.5 mGy/hour) over the 6-week HU period, resulting in a total dose of 0.5 Gy. A malfunction in the RT-PCR machine during our first set of analyses resulted in no data being acquired. Unfortunately, this caused a decrease in the number of samples available for subsequent analysis. The decrease in available samples resulted in it only being feasible to

make comparisons using a 2 x 2 factorial design of dietary iron level and hind limb unloaded state. The remaining treatment groups received the normal dietary iron and were cage controls (CC, n=3), or hind limb unloaded (HU, n=4), or they received the high iron diet (CC + Fe, n=4; HU + Fe, n=4). Gene targets of interest (TNF-α, and Slc5a8) were analyzed and the data normalized using 18S RNA. There were no significant changes in expression of TNF-α and Slc5a8 caused by the elevated iron diet or hind limb unloading or their interaction. Even though there were no significant differences, there is a demonstrated tendency for increased expression of TNF-α and Slc5a8 in all treatment groups, relative to the cage controls receiving the normal iron diet. These observations suggest the potential for these variables to have an impact on intestinal and systemic health of astronauts. More experiments with greater numbers of observations are necessary to explore the effects of radiation, diet, and weightlessness.

ACKNOWLEDGMENTS

I would like to thank my principal investigator Dr. Nancy Turner, Dr. Laurie Davidson and Dr. Susan Bloomfield, lab manager Elizabeth Petit, graduate students Derek Seidel, Kim Wahl, Michelle Summerfield, Shannon Lloyd, and Rihana Bokhari for their guidance and support throughout the course of this research.

Thanks also go to my friends, colleagues, and the department faculty of Veterinary and Biomedical Sciences for providing an environment of scholastic focus and achievement here at Texas A&M University.

CHAPTER I

INTRODUCTION

Radiation Insult

The inflammatory response and oxidative damage caused by ionizing radiation in space presents major concerns for the health of astronauts. Astronauts are exposed to high energy protons and ions (HZE), and low linear energy transfer rays (LET) from galactic cosmic rays while travelling in space. The difference between the types of radiation sources involves the amount of energy imparted from the radiation to the medium of passage per unit length [21].

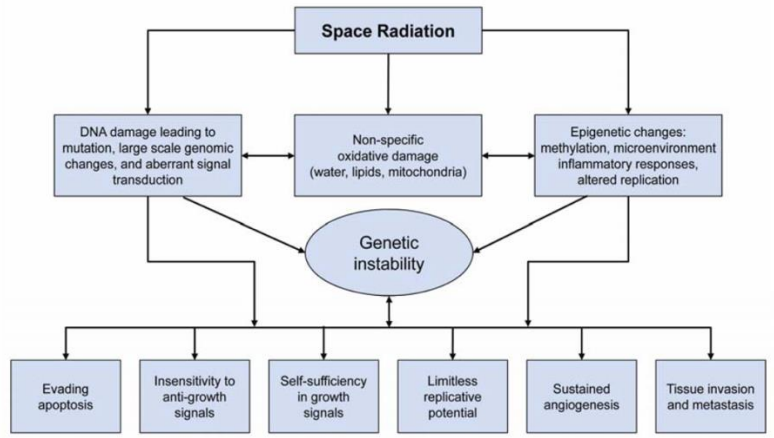

Figure 1. An overview of radiation damage effects observed leading to human cancer [6].

It has been shown that high-LET ^{56}Fe radiation produces more incidents of intestinal tumorigenesis of epithelial cells relative to low LET radiation [18]. Despite this, we know that ionizing radiation on earth does promote carcinogenesis [29]. Low LET radiation is known to alter the cell cycle, induce tumorigenesis by genomic instability and genetic mutations [5]. In addition, oxidative stress is elicited and found to have elevated reactive oxygen and nitrogen species, ROS and RNS respectively [30].

Microgravity

The experimental design allowed insight into the intestinal perturbation caused by microgravity [24]. Though not well studied in the colon, microgravity is known to alter fluid circulation, muscle atrophy, bone mineralization, and immune dysregulation [14, 22, 25]. It has been shown that mucosal cytokine levels in hind limb unloaded mice are altered by elevated IL-6 and suppressed IL-10 [24]. This altered homeostasis between pro- and anti- inflammatory cytokines, respectively, contribute to an overall pro-inflammatory state in the intestine.

Elevated Iron

High iron stores induced by increased dietary iron levels may stimulate reactive oxygen species (ROS) generation, which would contribute to oxidative stress [1]. Excessive ROS is known to increase cells sensitivity to radiation [2], and exposure to ionizing radiation also contributes to systemic oxidative stress [3]. Enhanced oxidative damage can result from the Fenton reaction, a reaction promoted by free iron ions, in which superoxide anions are converted to form highly reactive hydroxyl radicals. During the initial weeks of spaceflight, red blood cell numbers are decreased due to lysis, which also contributes to increased body iron stores [12]. Free radicals can also affect many metabolic processes, including those that regulate DNA, RNA, proteins, and lipids [15]. ROS produced from these processes and as a result of chronic inflammation can cause DNA damage, promote carcinogenesis, and long term immune system alteration [3].

Human- Microbe Symbiosis

The gastrointestinal tract hosts on the order of 10^{14} microorganisms that play a role in contributing or detracting from the overall health of the human host. The disruption of the human-microbe symbiotic relationship can eventually result in the risk of developing

Inflammatory Bowel Disease, Irritable Bowel Syndrome, diabetes, asthma, and cancer [20, 33]. The profile of an individual's microbial population is known to change over time according to alterations in diet, antibiotic intake, or injury such as radiation. Identification of the changes in bacterial population can be studied by the molecules produced by bacterial metabolism in the intestine.

As it relates to the colon, microbiota can use dietary fiber and starch polysaccharides as a source of energy and nutrient source for bacteria growth. Short Chain Fatty Acids (SCFAs), such as acetate, propionate, and butyrate, are produced by the fermentation of dietary fiber. Of the three, butyrate holds the most preventive potential in cancer by promoting cell cycle arrest, apoptosis, cell differentiation and suppressing colonic inflammation [32]. The link between health benefits and intake of dietary fiber by butyrate help to show the importance of this mechanism in colonic health.

It has been shown that butyrate is transported by a plasma membrane protein expressed by the gene Slc5a8 [34]. The protein transports butyrate into the cell where it acts to inhibit histone deacetylases (HDACs). HDACs serve to regulate the expression of proteins that regulate the cell cycle and progression of cancer [35, 36]. The lack of inhibition by butyrate explains recent findings that there is an inverse relationship between cancer incidence and levels of butyrate in the colon [37]. For these reasons, the Slc5a8 gene is defined as a tumor suppressor gene, usually silenced in colon cancer to evade apoptosis, or natural cell regulated death.

Inflammation in the Colon

Toll Like Receptors (TLRs) found in the epithelial tissues of the gastrointestinal tract function to recognize microbial pathogens and initiate an appropriate immune response. TLRs have been found to play a role in chronic inflammation by creating inflammatory mediators such

as TNF-α, IL-6, IL-10 [31]. Changes in cytokine levels is consistent with Irritable Bowel Diseases such as Crohn's disease or ulcerative colitis, often a precursor for intestinal cancer [27, 28].

CHAPTER II

METHODS

Diet

The AIN 93G diet was used for the duration of the study. The iron level in the control diets was provided by ferric citrate (45 mg iron/kg), which provided a level that satisfies mouse iron requirements. The high Fe diet included 650 mg iron/kg, which has been used by others to model a moderately high iron diet that results in increased oxidative damage [15]. The diet was introduced 4 weeks prior to starting the HU or C-RAD treatment.

Hind Limb Unloading

Mice were suspended using the tail ring method of Ferreira et al. [16]. The hind limb unloading model simulates weightlessness by maintaining a full body head down tilt. The mice underwent hind limb unloading for the 42 days, during which the same radiation treatment occurred.

Radiation Exposure

Continuous radiation (C-RAD) mice were exposed to a whole-body dose of ^{60}Cobalt gamma (γ) radiation on a continuous basis (0.5 mGy/hour) over the 6-week HU period, resulting in a total dose of 0.5 Gy. Activated cobalt wires were placed around a standard animal housing cage rack to provide continuous low level exposure.

Sample Collection

Procedures used for collection and analysis of scraped colon mucosa followed the procedures previously published by our lab [19,20]. Mice were euthanized by CO_2 asphyxiation followed by cervical dislocation. The colon was removed and luminal contents placed into a

cryotube and frozen in liquid nitrogen. The colon was flushed with RNase free PBS and cut in half longitudinally. One half was scraped to collect the mucosa that was used for gene expression analysis, and the other half processed for histological analysis. Mucosa was scraped from the colon on an RNase free surface (glass on ice) and transferred to an RNase free homogenization tube along with 250 µl of Denaturation solution (Ambion). Scraped mucosa was homogenized for at least six strokes and then transferred to a 2 mL eppitube for storage at -80°C.

Gene Expression

RNA from the colonic mucosal scraping was isolated using a ToTALLY RNA kit (Ambion, Austin, TX) followed by DNase treatment (DNA-free Kit, Ambion, Austin, TX). The concentrations of mRNA were collected using spectrophotometry nanodrop. RNA quality was checked using an Agilent 2100 Bioanalyzer with nanochips or picochips depending on the concentration of RNA (RNA 6000 Nano LabChip). Expression of TNF-α, IL-6, IL-10, and Slc5a8 were analyzed via real time PCR using TaqMan Array plates and a ABI7900 HT real-time thermocycler. Control genes of 18S and GAPDH were used to normalize results. PCR conditions were as follows:

UDG Incubation	2 min	50° C
AmpliTaq, Gold, UP Activation	10 min	95° C
PCR (40 Cycles)		
Denature	15 sec	95° C
Anneal/Extend	1 min	60° C

Table 1. Target and control gene assay information

Gene Symbol	Catalog Number	TaqMan Assay ID
TNF-α	4331182	Mm00443258_m1
IL-6	4331182	Mm00446190_m1
IL-10	4331182	Mm01288386_m1
Slc5a8	4331182	Mm00520629_m1
GAPDH	4331182	Mm99999915_m1
18S	4331182	Mm03928990_m1

Preliminary Experiment

The amount of input cDNA (100 ng, 10 ng, 1 ng, 0.1 ng) was tested in a preliminary RT-PCR reaction to identify the most appropriate amount of cDNA for each gene target. Based on cycle threshold values for all tested genes above, only TNF-α and Slc5a8 produced sufficiently repeatable results. IL-6 and IL-10 were not used as a gene of interest in further expression analysis.

Statistical Methods

Results from the RT- PCR analyses were derived using the comparative C_t method for relative quantifications [38]. The data were analyzed using the General Linear Model (GLM) with the SAS (version 9.4) program. The samples were tested for differences in main effects and interaction effects due to diet, hind limb unloading, and radiation.

CHAPTER III

RESULTS AND CONCLUSION

Results

The amount of mRNA isolated from the colon scraped mucosa samples was determined to calculate the amount of starting material to reverse transcribe in to cDNA in later steps. Table 1 in Appendix A holds the spectrophotometry and RNA quality data for all samples. Nucleic acid absorbance maximums are at 260nm and 280nm, and phenol or protein contamination produce a signal at 230nm. The 260/280 absorbance ratio is used to determine the purity of the nucleic acids present, where acceptable ratios are between 1.8 and 2.0. The 260/230 ratio is an assessment used to determine phenol contamination, with acceptable ratios commonly being between 2.0 and 2.2. The observed 260/280 mean was 1.945 ± 0.155 and the 260/230 ratio mean was 0.640 ± 0.437.

The Agilent Bioanalyzer produced the RNA Integrity Number (RIN) which demonstrated a secondary sense of quality of RNA in addition to spectrophotometry. A RIN is generated by the detected 18s and 28s RNA peaks, and is a quantifiable measure of the degradation caused by RNase enzymes. Shorter fragments of degraded RNA can compromise gene expression analysis. Acceptable sample RIN result is between 8 and 10, therefore any sample with a RIN value below 8.0 was not used in later steps of analysis. The Agilent RNA 6000 Nano Kit Guide pictures the peaks expressed by the reaction below (Figure 2).

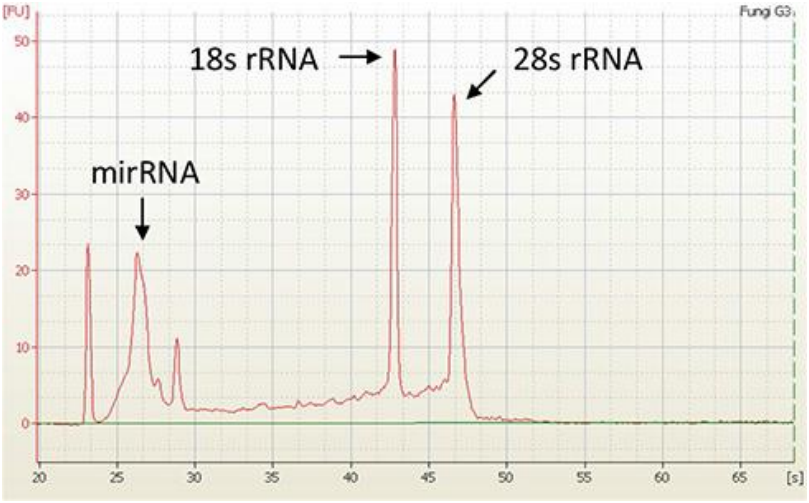

Figure 2. Factors in analysis of RNA quality

Gene Expression by RT-PCR

The RT-PCR runs were not usable because of a malfunction in the ABI7900 HT real-time thermocycler. A follow up experiment was conducted using a Roche 480 machine to obtain results. Not all samples could be used in the follow up experiment due to a limited amount of initial RNA available. All cycle threshold data can be found in Table 2 in Appendix A. The decrease in available samples for data analysis meant we were only able to compare results from a 2 x 2 factorial design of altered diet and hind limb unloaded state with CC (n=3), HU (n=4), CC + Fe (n=4), and HU + Fe (n=4).

The mean expression of TNF-α in the scraped colon mucosa from the cage control mice was 1.920 ± 1.881 (Table 2, Figure 3). The expression of TNF-α in all other treatment groups tended to be higher (HU is a 203%, CC + Fe is a 185%, and HU + Fe is a 207% increase). The expression of Slc5a8 in the scraped colon mucosa was also lower in the cage control mice (Figure 4). Increasing dietary iron or incorporating hind limb unloading also tended to increase expression of Slc5a8 (HU is a 789%, CC + Fe is a 1184%, HU + Fe is a 846% increase).

Table 2. Changes in gene expression in the colon relative to 18S							
	High Fe		**Normal Fe**		**Main Effect P values**		**Interaction effects P values**
Gene	CC	HU	CC	HU	Diet	HU	Diet + HU
TNF-α	3.550 ± 1.330	3.975 ± 1.330	1.920 ± 1.881	3.888 ± 1.330	0.224	0.226	0.224
Slc5a8	1.504 ± 0.612	1.074 ± 0.612	0.127 ± 0.865	1.002 ± 0.612	0.491	0.319	0.463

Values are least squares means with standard error of the mean for each gene. Data are presented relative to the expression of reference gene (18S). P values are included for main effects and interaction effects.

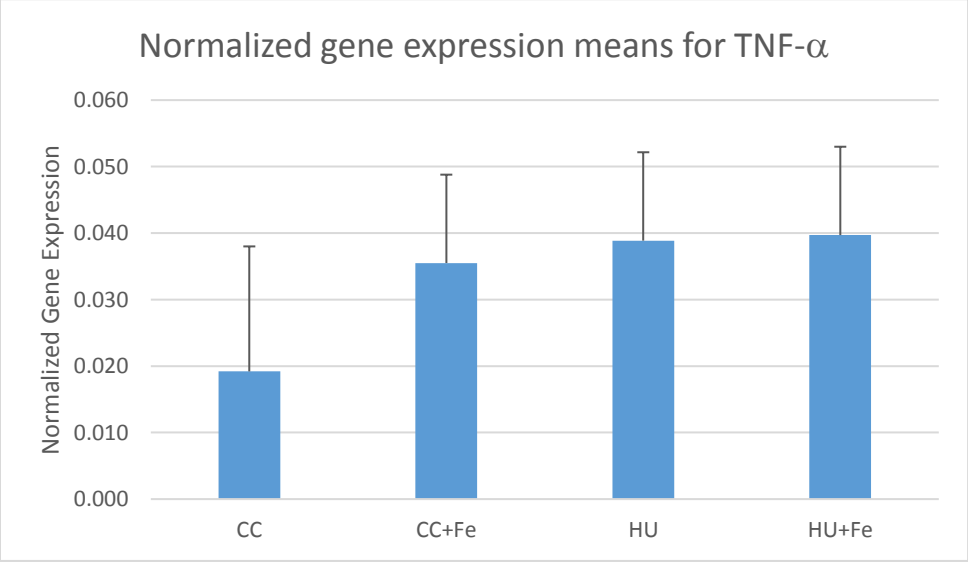

Figure 3. Gene expression for TNF-α normalized to 18S

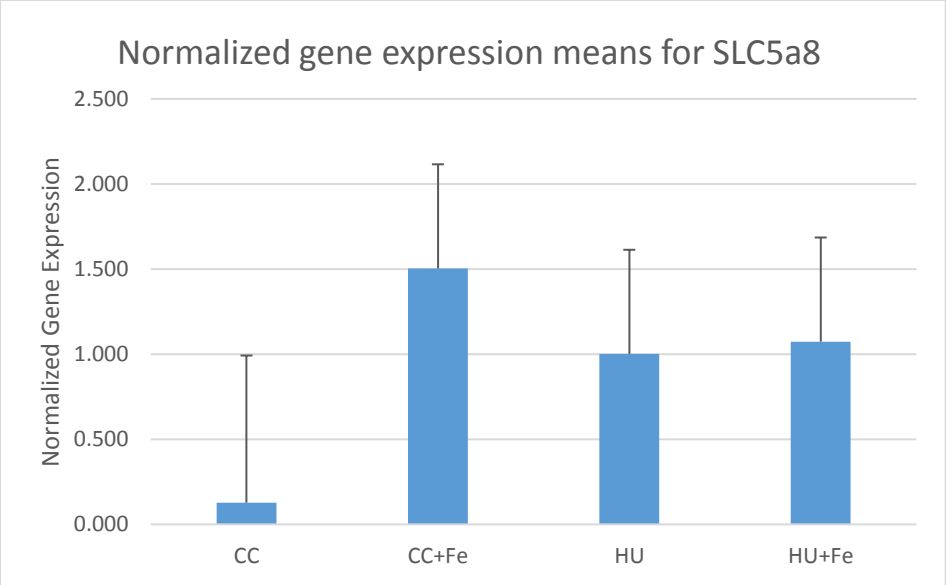

Figure 4. Gene expression for Slc5a8 normalized to 18S

Discussion

A previous study using rats demonstrated that as the levels of oxidative stress and inflammatory tone in the colon increased in response to elevated dietary iron and low LET radiation, the expression of several genes involved in inflammation and SCFA transport also changed [(19)]. That research suggests the expression of Slc5a8 should be lower and that of TNF-α should be higher relative to a weight bearing and normal iron diet control in this experiment [(19)]. Figure 3 and 4 document an overall tendency for an increase expression of TNF-α and Slc5a8 of mice given either elevated iron diets or are hind limb unloaded, relative to the low dietary iron cage control mice. This tendency is reflective of alterations in gene expression reported to occur in response to diet and microgravity experienced by astronauts in space [(14)]. The small sample numbers available for this work prohibited our ability to detect treatment differences. However, the pattern of responses observed suggests that these treatments may induce meaningful changes in the intestine.

In colorectal cancer, Slc5a8 is known to be a tumor suppressor gene and is usually down regulated in colon cancer, whereas TNF-α upregulation in colon mucosa is associated with increased CRC incidence [37, 39]. Recent research has explored potential drug therapies for inhibition of TNF-α to prevent the growth of tumors in CRC [40]. The effect of these two variables on the expression of these genes may be contributing to the incidence of CRC in astronauts. The Longitudinal Study of Astronaut Health has determined that a diagnosis of benign or malignant neoplasm incidence is occurring at a higher rate compared to a group of comparison participants [41].

Conclusion

Using a high iron diet or hind limb unloading to model the spaceflight environment did not produce statistically significant changes of colonic gene expression of TNF-α and Slc5a8 in this experiment. Variability in the animal responses in combination with low sample numbers precludes our ability to detect significant differences. However, there is a demonstrated tendency for increased expression of TNF-α and Slc5a8 with either an increase in dietary iron or with hind limb unloading. These preliminary observations suggest these space-relevant variables may contribute to immunological perturbations of the intestine mucosa and the altered relationship between gut microbiota and the human host. These changes may impact colon and overall health of the astronauts during spaceflight.

The results would be improved in future experiments with larger sample numbers. More experiments will be necessary to explore the effects of radiation, diet, and weightlessness to model the astronaut environment. Future research can expand the scope of genes of interest to other inflammatory pathways that are involved in colon health.

REFERENCES

1. Li M, Gonon G, Buonanno M, Autsavapromporn N, de Toledo SM, Pain D, Azzam EI. Health risks of space exploration: targeted and nontargeted oxidative injury by high-charge and high-energy particles. Antioxid Redox Sign. 2014;20:1501-1523.

2. Dayal R, Singh A, Pandey A, Mishra KP. Reactive oxygen species as mediator of tumor radiosensitivity. J Canc Res Ther. 2014;10:811-818.

3. Kennedy AR, Guan J, Ware JH. Countermeasures against space radiation induced oxidative stress in mice. Radiat Environ Biophys. 2007;46:201-203.

4. Chang ML, Hou JK. Cancer risk related to gastrointestinal diagnostic radiation exposure. Curr Gastroenterol Rep. 2011;13:449–57.

5. BEIR. Committee to Assess Health Risks from Exposure to Low Levels of Ionizing Radiation. National Research Council of the National Academies: Health risks from exposure to low levels of ionizing radiation. BEIR VII – Phase 2. The National Academies Press, Washington, D.C. 2006.

6. Hanahan D, Weinberg RA. The hallmarks of cancer. Oxford Textbook of Oncology. 2016;3–10.

7. Li H, Myeroff L, Smiraglia D, Romero MF, Pretlow TP, Kasturi L, et al. SLC5A8, a sodium transporter, is a tumor suppressor gene silenced by methylation in human colon aberrant crypt foci and cancers. Proc Natl Acad Sci USA. 2003;100:8412–8417.

8. Ullman TA, Itzkowitz SH. Intestinal inflammation and cancer. Gastroenterology. 2011; 140:1807-1816.

9. Tang WH, Wang Z, Levison BS, Koeth RA, Britt EB, Fu X, Wu Y, Hazen SL. Intestinal microbial metabolism of phosphatidylcholine and cardiovascular risk. N Engl J Med 2013;368:1575-1584.

10. Noor SO, Ridgway K, Scovell L, Kemsley EK, Lund EK, Jamieson C, et al. Ulcerative colitis and irritable bowel patients exhibit distinct abnormalities of the gut microbiota. BMC Gastroenterol. 2010;10:134

11. Sepehri S, Kotlowski R, Bernstein CN, Krause DO. Microbial diversity of inflamed and noninflamed gut biopsy tissues in inflammatory bowel disease. Inflamm Bowel Dis. 2007;13:675-683.

12. Alfrey CP, Udden MM, Leach-Huntoon C, Driscoll T, Pickett MH. Control of red blood cell mass in spaceflight. J Appl Physiol. 1996;81:98-104.

14. Globus RK, Morey-Holton E. Hindlimb unloading: rodent analog for microgravity. J Appl Physiol. 2016;120:1196-1206.

15. Fischer JG, Glauert HP, Yin T, Sweeney-Reeves ML, Larmonier N, Black MC. Moderate iron overload enhances lipid peroxidation in livers of rats, but does not affect NF-kappaB activation induced by the peroxisome proliferator. J Nutr. 2002;132:2525-31.

16. Ferreira JA, Crissey JM, Brown M. An alternant method to the traditional NASA hindlimb unloading model in mice. J Vis Exp. 2011l;49.

17. Datta K, Suman S, Kallakury BV, Fornace AJ, Jr. Exposure to heavy ion radiation induces persistent oxidative stress in mouse intestine. PLoS One. 2012; 10.1371/journal.pone.0042224.

18. Trani D, Datta K, Doiron K, Kallakury B, Fornace AJ, Jr. Enhanced intestinal tumor multiplicity and grade in vivo after HZE exposure: mouse models for space radiation risk estimates. Radiat Environ Biophys. 2010;49:389-396.

19. Morgan JL, Ritchie LE, Crucian BE, Theriot C, Wu H, Sams C, Smith SM, Turner ND, Zwart SR. Increased dietary iron and radiation in rats promote oxidative stress, induce localized and systemic immune system responses, and alter colon mucosal environment. FASEB J. 2014;28:1486-1498.

20. Ritchie LE, Taddeo SS, Weeks BR, Lima F, Bloomfield SA, Azcarate-Peril MA, Zwart SR, Smith SM, Turner ND. Space Environmental Factor Impacts upon Murine Colon Microbiota and Mucosal Homeostasis. PLoS One. 2015; 10.1371/journal.pone.0125792.

21. Friedberg W, Copeland K. Ionizing Radiation in Earth's Atmosphere and in Space Near Earth. 2011.

22. Morey-Holton ER, Globus RK. Hindlimb unloading rodent model: technical aspects. Journal of Applied Physiology. 2002;92:1367-1377

23. Zheng, et al. Gene expression profiling in non-human primate jejunum, ileum and colon after total-body irradiation: a comparative study of segment-specific molecular and cellular responses. BMC Genomics. 2015;16:984.

24. Li P, Shi J, Zhang P, Wang K, Li J, Liu H, Zhou Y, Xu X, Hao J, Sun X et al. Simulated microgravity disrupts intestinal homeostasis and increases colitis susceptibility. FASEB J. 2015;29:3263-3273.

25. Williams D, Kuipers A, Mukai C, Thirsk R. Acclimation during space flight: effects on human physiology. CMAJ. 2009;180:1317-1323.

26. Smith SM, Zwart SR. Nutritional Biochemistry of Spaceflight: Advances in Clinical Chemistry. 2008;87–130.

27. Neurath MF. Cytokines in inflammatory bowel disease. Nat Rev Immunol. 2014;14:329–342.

28. Andoh A, Yagi Y, Shioya M, Nishida A, Tsujikawa T, Fujiyama Y. Mucosal cytokine network in inflammatory bowel disease. World J of Gastroenterolo. 2008;14:5154-5161.

29. Brenner DJ, Hricak H. Radiation exposure from medical imaging: time to regulate? JAMA. 2010;304:208–209.

30. Baulch JE, Craver BM, Tran KK, Yu L, Chmielewski N, Allen BD, Limoli CL. Persistent oxidative stress in human neural stem cells exposed to low fluences of charged particles. Redox Biol. 2015;24–32.

31. Drexler SK, Foxwell BM. The role of toll-like receptors in chronic inflammation. Int J Biochem Cell Biol. 2010;42:506-18.

32. Ganapathy V, Thangaraju M, Prasad PD, Martin PM, Singh N. Transporters and receptors for short-chain fatty acids as the molecular link between colonic bacteria and the host. Curr Opin Pharmacol. 2013;13:869-874.

33. Derrien M, Veiga P. Rethinking Diet to Aid Human-Microbe Symbiosis. Trends Microbiol. 2017;25:100-112.

34. Thangaraju M, Cresci G, Itagaki S, Mellinger J, Browning DD, Berger FG, Prasad PD, Ganapathy V. Sodium-coupled transport of the short chain fatty acid butyrate by SLC5A8 and its relevance to colon cancer. J Gastrointest Surg. 2008;12:1773-1781; discussion 1781-1772.

35. Chen JS, Faller DV, Spanjaard RA. Short-chain fatty acid inhibitors of histone deacetylases: promising anticancer therapeutics? Curr Cancer Drug Targets. 2003;3:219-236.

36. Glozak MA, Seto E. Histone deacetylases and cancer. Oncogene. 2007;26:5420-5432.

37. World Cancer Research Fund, American Institute for Cancer Research. Food, Nutrition, Physical Activity, and the Prevention of Cancer: a Global Perspective. Washington DC. AICR. 2007.

38. Schmittgen TD, Livak KJ. Analyzing real-time PCR data by the comparative C_T method. Nature Protocols. 2008; 1101-1108.

39. Al Obeed OA, Alkhayal KA, Al Sheikh A, et al. Increased expression of tumor necrosis factor-α is associated with advanced colorectal cancer stages. WJG. 2014;20:18390-18396.

40. Zidi I, Mestiri S, Bartegi A, Amor NB. TNF-alpha and its inhibitors in cancer. Med Oncol. 2010;27:185–198.

41. National Aeronautics and Space Administration. Colorectal Cancer Incidence of LSAH Participants. In: Longitudinal Study of Astronaut Health Newsletter. December 1999;8:2.

APPENDICES

Appendix A -Experiment Data

Table 1. Spectrophotometry and RNA quality data for all experimental mice

Animal ID	**Design**	**Concentration (ng/ul)**	**260/280 ratio**	**260/230 ratio**	**RNA Integrity Number (RIN)**
1102	CC	70.12	2.06	0.26	10
1106	CC	134.29	2.03	1.68	10
1206	CC	12.27	1.72	0.24	9.6
1208	CC	35.16	1.87	0.51	2.4
1211	CC	3.74	1.61	0.06	7.9
1218	CC	24.02	1.77	0.24	10, 8
1219	CC	56.36	1.74	0.75	9.8
1222	CC	27.6	1.87	0.36	8.6
1223	CC	36.11	1.86	1.07	2.4
1230	CC	75.65	1.95	0.45	10
1233	CC	45.93	1.92	0.39	9.8
1234	CC	43.42	1.96	0.71	9.8
1235	CC	10.11	1.94	0.26	5.5
1107	CC+Fe	96.77	1.97	1.02	9.8
1108	CC+Fe	81.91	1.98	1	9.8
1109	CC+Fe	167.86	2.01	1.53	10
1110	CC+Fe	107.75	2.05	1.82	9.9
1111	CC+Fe	143.32	2.03	0.46	9.9
1112	CC+Fe	162.67	2.03	1.81	9.9
1114	CC+Fe	82.49	2	0.72	10
1214	CC+Fe	34.37	1.96	0.39	6.4
1216	CC+Fe	37.16	1.9	0.65	-

1225	CC+Fe	32.06	2.01	0.37	9.1
1228	CC+Fe	24.46	1.92	0.34	9.2
1229	CC+Fe	43.25	1.97	0.36	5.1
1101	HU	149.97	2.03	1.7	10
1104	HU	132.22	2.01	0.94	10
1105	HU	131.78	2.02	1.08	10
1207	HU	40.02	1.88	0.61	8.4
1209	HU	62.94	1.98	0.41	9.7
1210	HU	28.13	2.08	0.22	8.9
1220	HU	17.99	1.86	0.13	9.5
1221	HU	86.26	2.01	0.69	9.9
1231	HU	52.3	1.9	0.56	10
1232	HU	34.27	1.98	0.39	9.5
1103	HU	106.19	2.03	1.28	8.7
1113	HU+Fe	117.03	2.01	1.24	9.9
1115	HU+Fe	3.46	1.72	0.06	1.1
1201	HU+Fe	42.52	1.97	0.7	10
1203	HU+Fe	40.45	1.91	0.58	
1204	HU+Fe	51.95	2.02	0.2	10
1205	HU+Fe	44.64	2.04	0.94	9.3
1212	HU+Fe	71.75	1.63	0.43	9.8
1213	HU+Fe	57.96	1.95	0.68	9.9
1224	HU+Fe	41.29	1.87	0.61	2.4, 5.8
1227	HU+Fe	70.84	1.76	0.52	10
1800	Rad	165.55	1.55	0.6	5.2
1801	Rad	24.66	1.65	0.25	4.3
1808	RadFe	49.92	2.05	0.93	6.9
1809	RadFe	9.22	2.06	0.13	8.1
1810	RadFe	56.82	1.64	0.58	9.2
1811	RadFe	23.65	2.11	0.15	9.1, 5.3

1812	RadFeHU	27.3	2.03	0.45	8
1813	RadFeHU	37.89	2	0.78	2.4
1814	RadFeHU	45.87	1.98	0.36	5.6
1815	RadFeHU	15.63	2.15	0.52	2.7, 5.7
1816	RadFeHU	53.52	1.68	0.53	1
1817	RadFeHU	26.19	2.1	0.45	10
1818	RadFeHU	40.41	2.01	1.1	7.6
1819	RadFeHU	46.04	1.86	0.52	8.4
1820	RadFeHU	37.75	2.05	0.66	5.5
1821	RadFeHU	11.99	1.94	0.21	5.9
1802	RadHU	17.42	2.07	0.69	4.6
1803	RadHU	3.9	2.62	0.07	8.9
1804	RadHU	25.21	1.96	0.89	7.8
1805	RadHU	78.97	2.05	1.63	7.9
1806	RadHU	26.8	1.89	0.42	9.7
1807	RadHU	16.63	2.04	0.17	10, 2

Table 2. Cycle Threshold Data for all Experimental Samples						
Animal ID	Design	Triplicate CT values	Gene			
			TNF-α	**Slc5a8**	**GAPDH**	**18S**
1219[1]	CC					
		1	38.88	34.83	34.54	31.67
		2	36.92	33.76	33.36	31.76
		3	36.98	33.86	33.89	31.7
1233[1]	CC					
		1	41.53	40.65	37.89	36.33
		2	40.83	39.83	38.29	36.16
		3	42.4	39.16	37.19	35.65
1234[1]	CC					
		1	39.47	39.14	41.94	42.93
		2	38.67	37.47	-----	40.6
		3	38.64	37.62	-----	41.39
1107[1]	CC+Fe					
		1	34.85	28.96	30.02	31.04
		2	35.57	29.7	30.07	30.97
		3	34.94	29.71	30.67	31.17
1110[1]	CC+Fe					
		1	33.38	28.23	27.45	28.08
		2	33.54	27.29	29.68	29.96
		3	33.99	27.86	28.5	27.86
1111[1]	CC+Fe					
		1	33.38	28.87	-----	27.71
		2	33.33	28.71	28.74	28.33
		3	33.3	28.85	29.88	27.54
1112[1]	CC+Fe					
		1	32.33	28.19	28.07	27.98
		2	32.66	28.25	28.48	27.78

		3	34.27	29.12	27.83	28.07
1101[1]	HU					
		1	33.4	29.54	29.57	29.57
		2	33.84	28.67	30.03	29.63
		3	32.7	29.27	28.89	28.83
1104[1]	HU					
		1	34.71	28.6	30.01	29.73
		2	34.86	29.38	29.39	29.93
		3	35.11	29.26	30.94	30.87
1209[1]	HU					
		1	34.31	30.8	30.52	28.86
		2	34.48	31.09	29.93	28.89
		3	34.91	30.42	30.75	32.7
1221[1]	HU					
		1	39.89	35.85	34.97	31.88
		2	38.55	35.85	34.8	32.51
		3	39.87	35.9	34.9	32.39
1231[2]	HU					
		1	-----	-----	41.93	37.01
		2	-----	-----	41.35	40.21
		3	-----	-----	-----	40.6
1113[1]	HU+Fe					
		1	33.85	28.42	29.1	29.45
		2	34	28.71	28.85	30.98
		3	33.35	28.26	29.08	30.49
1205[1]	HU+Fe					
		1	33.89	29.95	28.32	27.62
		2	33.64	31.97	28.47	27.94
		3	33.67		28.73	27.97
1212[1]	HU+Fe					
		1	39.72	36.29	35.64	31.92

		2	39.45	36.56	35.88	31.87
		3	38.84	37.09	36.37	32.03
1213[1]	HU+Fe					
		1	32.52	29.08	30.18	27.92
		2	32.9	28.48	30.2	28.32
		3	32.85	29.67	30.36	28.43
1808[1]	RadFe					
		1	35.88	32	31.98	33.58
		2	35.98	31.83	32.73	27.83
		3	35.92	32.09	32.47	28.72
1810[2]	RadFe					
		1	-----	42.74	35.04	36.86
		2	-----	-----	39.68	37.81
		3	-----	-----	35.53	37.24
1818[2]	RadFeHU					
		1	-----	-----	-----	42.27
		2	-----	-----	-----	40.82
		3	-----	-----	-----	-----
1819[2]	RadFeHU					
		1	-----	-----	40.54	41.64
		2	-----	-----	41.84	41.45
		3	-----	-----	41.93	42.71

Table 2. Cycle Threshold Data for all Experimental Samples. [1]Samples were included for statistical analysis. [2]Samples were not included in statistical analysis due to absence of cycle threshold output generated during RT- PCR.

Appendix B -Experimental Protocols

Mucosal mRNA Isolation

RNAqueous Kit (Applied Biosystems #AM1912)

Handle all samples in RNase free conditions, including sample tubes, gloves, equipment etc.

Prior to starting, heat 50 ul (per sample) aliquot of Elution Solution at 75° C.

Reduce the viscosity of the lysate if necessary, ensure tissue is well homogenized. Use 25 gauge syringe needle to break up lysate.

1- Add equal volume of 64% ethanol to the lysate and mix gently

2- Apply the mixture from previous step to a filter cartridge in a supplied collection tube (max volume that can be applied is 700 ul)

3- Centrifuge at RCF 10,000-15,000 x g for 1 minute, or until lysate/ethanol has passed through the filter

4- Discard flow through and keep collection tube

5- Repeat step 3 as necessary until all the sample has been drawn through the filter. Add up to 700 ul 64% ethanol as necessary.

6- Apply 700 ul Wash Solution #1 to the filter cartridge

7- Centrifuge at RCF 10,000-15,000 x g for 1 minute, or until lysate/ethanol has passed through the filter. Discard flow through and keep collection tube

8- Add 500 ul Wash Solution 2/3

9- Centrifuge at RCF 10,000-15,000 x g for 1 minute, or until lysate/ethanol has passed through the filter. Discard flow through and keep collection tube

10- Repeat steps 8 and 9

11- Put filter cartridge into a fresh Collection Tube

12- Pipet preheated Elution Solution to the center of the filter (40 ul)
13- Recover by centrifugation for 30 seconds at same speed above
14- Repeat step 12 with only 10 ul Elution Solution

Store isolated RNA in -80° C freezer conditions

Post Isolation DNase Treatment for RNA

Catalog Number: AM1912

1- Add 0.1 Volume (for 50 ul elution → 5 ul) 10X DNase 1 Buffer and 1 ul rDNase 1 to the RNA, and mix gently
2- Incubate at 37° C for 20-30 minutes.
3- Add re suspended DNase Inactivation Reagent (typically 0.1 volume → 5.5 ul) and mix well
4- Incubate 2 min at room temperature, mixing occasionally
5- Centrifuge at 10,000 x g for 1.5 min and transfer the RNA to a fresh RNAse free tube.
6- Aliquot 4 ul into RNase free PCR tube for Nanodrop and Agilent QC.

Tubes needed:
Filter Cartridge x1 per sample
Collection Tube x2 per sample
.65 ml RNase free tube x1 per sample (for post DNAse treatment collection)
RNase free PCR Tube x1 per sample (for ND and Agilent aliquot)

Spectrophotometry via Nanodrop for RNA

1- Clean the upper and lower optical surfaces of the microspectrophotometer. Pipet 1 to 2 ul of clean deionized water to clean the system
2- Open the NanoDrop software and select the nucleic acids module
3- Initialize the spectrophotometer by placing 1 ul of clean water onto the lower optical surface, lowering the arm and selecting “initialize” in the software.
4- Clean surface by wiping with Kimwipe
5- Measure the nucleic acid sample by loading 1 ul and select “measure.”
6- Record the concentration of nucleic acid I ng/ul and the ratios at 260/230 and 260/280

Measuring RNA Quality

1. Put ~5 µL of each sample in a labeled eppitube and place on ice.
3. Analyze samles on a NanoChip using and Agilent 2100 Bioanalyzer using complementary software.

a. Make sure Bioanalyzer is connected to computer and power source.
b. Turn on Bioanalyzer, make sure indicator light is green.
c. Start Agilent 2100 Bioanalyzer software.
d. Select Assay>RNA>mRNA nano
e. Prepare samples, buffer, and nano chip. (See RNA 6000 Nano LabChip kit)
f. Place chip in Bioanalyzer and close lid.
g. Click "Start" above the chip icon.
h. Ensure that sample names are all entered in the "Sample Information" tab.
i. Change File Prefix and click "Start."
j. When the run is finished, clean as indicated by the See RNA 6000 Nano LabChip kit.
k. Print Data.

NOTES:

RNA Integrity Number (RIN)
>9 is optimal
>8 is acceptable, if no errors are seen on the curve

• Prepare and run chips within 10 minutes. Longer chip preparation times may lead to evaporation of buffers and to bad chip performance.
• Vortex chips for appropriate 1 minute (not required for protein chips). Improper vortexing can lead to poor results.
• Do not force the chip into the receptacle of the Agilent 2100 Bioanalyzer. Proper placement of the chip should not require force. Improper placement of the chip could damage the electrode assembly when you close the lid. Check whether the chip selector is in the correct position.
• Do not touch wells of the chip. The chip could become contaminated, leading to poor measurement results.
• Do not leave any wells of the chip empty or the assay will not run properly. Add 1 µL of sample buffer to each unused sample well.

(From Thesis by Leigh Ann Piefer and methods done previously in this lab)

SuperScript III First Strand Synthesis System for RT-PCR

Catalog Number: 18080051

1- Mix and centrifuge samples before conducting assay
2- Combine the following in a 0.5 ul collection tube

- Up to 5 ug total RNA
- Primer
    - 50 uM oligo$(dT)_{20}$ 1 ul

3- Incubate the tube at 65° C for 5 min, then place on ice for at least 1 min,
4- Prepare the following cDNA synthesis mix

10X RT buffer	2 ul
25 mM $MgCl_2$	4 ul
0.1 M DTT	2 ul
RNaseOUT	1 ul
Superscripts III RT	1 ul

5- Add the 10 ul of synthesis mix to the RNA mix and collect by brief centrifugation. Incubate at 50° C for 50 minutes.
6- Terminate the reaction at 85° C for 5 minutes. Chill on ice.
7- Add 1 ul RNase H and incubate the tubes at 37° C for 20 minutes

Store in -20 freezer or for PCR immediately

Serial Dilutions for Practice RT-PCR using practice mice

100 ng cDNA:
In one tube add 1.06 x 8 (8.48) ul cDNA and 7.94 x 8 (63.52) ul H20
10 ng cDNA:
Add 1 x 8 (8) ul of the tube from above to 9 x 8 (72) ul of H20
1 ng cDNA
Add 1 x 8 (8) ul of the tube from above to 9 x 8 (72) ul of H20
0.1 ng cDNA
Add 1 x 8 (8) ul of the tube from above to 9 x 8 (72) ul of H20

TaqMan Gene Expression Master Mix

Catalog Number: 4369016

1- Start SDS program and ABI 7900 HT, allow time to heat and initialize
2- Pipet all components in the chart below into 96 well plate

Component	Volume (ul)

TaqMan Gene Expression Master Mix	10
TaqMan Gene Expression Assay	1
cDNA template +H_20	9
total	20

3- Run the PCR Plate using the “standard” cycling conditions

UDG Incubation	2 min	50° C
AmpliTaq, Gold, UP Activation	10 min	95° C
PCR (40 Cycles)		
Denature	15 sec	95° C
Anneal/Extend	1 min	60° C